1 Chart
5 Figures
4 Schemes
1 Table

Stereoelectronic Effects in C-H Bond Oxidation Reactions of Ni(I) N-Heterocyclic Carbene Complexes

Rebecca C. Poulten,[a] Isidoro López,[b] Antoni Llobet,[b] Mary F. Mahon[a] and Michael K. Whittlesey[a,*]

[a]*Department of Chemistry, University of Bath, Claverton Down, Bath BA2 7AY, UK and*

[b]*Institute of Chemical Research of Catalonia (ICIQ), Avinguda Paisos Catalans 16, E-43007 Tarragona, Spain*

Abstract

Activation of O_2 by the three-coordinate Ni(I) ring-expanded N-heterocyclic carbene complexes Ni(NHC)(PPh_3)Br (NHC = 6-Mes, 7-Mes) produced the dimeric Ni(II) complexes Ni(6-Mes)(Br)(μ-OH)(μ-O-6-Mes′)NiBr (**3**) and Ni(7-Mes)(Br)(μ-OH)(μ-O-7-Mes′)NiBr (**4**) containing oxidized *ortho*-mesityl groups from one of the carbene ligands. Mass spectrometry was consistent with bis-μ-aryloxy compounds also being formed in these reactions. Low temperature UV-visible spectroscopy showed that the reaction between Ni(6-Mes)(PPh_3)Br and O_2 was too fast even at ca. -80 °C to yield any observable intermediates. Addition of O_2 to Ni(I) precursors containing a less donating diamidocarbene (6-MesDAC) or the less bulky 6-/7-membered ring diaminocarbene ligands (6-/7-*o*-Tol) proceeded quite differently, affording phosphine and carbene oxidation products (Ni(O=PPh_3)$_2$$Br_2$ and (6-MesDAC)=O) and mononuclear dibromido Ni(II) complexes (Ni(6-/7-*o*-Tol)(PPh_3)Br_2) respectively.

Introduction

The activation of gaseous small molecules by Ni containing complexes is fundamental to a number of bioinorganic transformations. Thus, carbon monoxide is transformed during the action of acetyl coenzyme A synthase[1] and CO dehydrogenase,[2] dihydrogen by [NiFe] hydrogenase[3] and O_2 by nickel superoxide dismutase[4] and acireductone dioxygenase.[5] Efforts to further the understanding of Ni promoted oxidation chemistry have employed Ni model complexes and focussed on reactions of Ni(II) compounds with H_2O_2[6-8] or Ni(I) species with O_2 itself.[9-11] This latter approach is of particular interest given the importance often attached to Ni(I) as a key oxidation state,[12] although wide-ranging studies have been restricted by the lack of suitable ligand sets capable of stabilizing well-defined Ni(I) precursors.[11,13,14]

We have recently shown that N-heterocyclic carbene (NHC) ligands based on 6-, 7- and 8-membered rings (Chart 1) and containing bulky N-aryl substituents allow access to three-coordinate Ni(I) complexes of the general formula Ni(NHC)(PPh_3)X (X = Br, Cl).[15,16] In preliminary observations, we found that inadvertent exposure of yellow

solutions of these highly air-sensitive compounds to air resulted in extremely rapid changes of color to purple. We now report that for the 6- and 7-membered ring N-mesityl derived complexes, these color changes arise as a result of O_2 activation and formation of dimeric Ni(II) complexes containing NHCs that have undergone oxidation at an *ortho*-methyl C-H group.[17] We also show that Ni(I) precursors bearing either a less electron-rich diamidocarbene (DAC) ligand or a less bulky *ortho*-tolyl N-substituted 6- and 7-membered ring diaminocarbene also react with O_2 to give Ni(II) products, but that mononuclear species are formed as a result of phosphine oxidation or halide redistribution reactions.

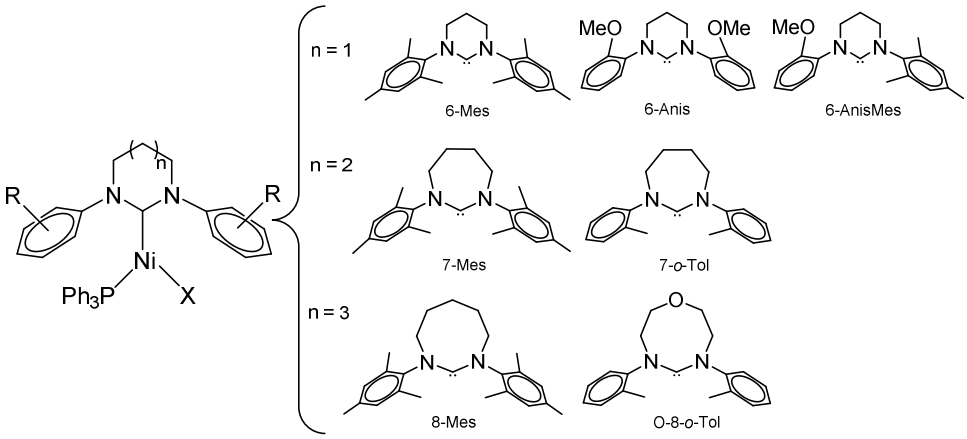

Chart 1

Experimental

All manipulations were carried out using standard Schlenk, high vacuum and glovebox techniques using dried and degassed solvents. NMR spectra were recorded in C_6D_6 (referenced to δ 7.15 and 128.0), CD_2Cl_2 (δ 5.32 and 54.5) and $CDCl_3$ (δ 7.24) on Bruker Avance 400 and 500 MHz NMR spectrometers. ^{31}P NMR spectra were

referenced to 85% H_3PO_4 at δ 0.0. UV-Visible spectroscopy was performed on a CARY 50 (Varian) UV-visible spectrophotometer using an all-quartz immersion probe with 1 cm optical path length from Hellma. The temperature was kept constant at -83 °C by means of a liquid N_2/acetone bath and monitored by a low-temperature thermometer. Kinetic data were processed by use of the program SPECFIT/32 Global Analysis System, which uses the method of Singular Value Decomposition (SVD). Mass spectra were recorded on a Bruker MicrOTOF electrospray time-of flight (ESI-TOF) mass spectrometer (Bruker Daltonik GmbH) coupled to an Agilent 1200 LC system (Agilent Technologies). Elemental analyses were performed by the Elemental Analysis Service, London Metropolitan University, London, UK. Complexes **1**, **2**, **9** and 6-MesDAC, were prepared according to the literature.[16,18] $Ni(cod)_2$ and $Ni(PPh_3)_2Br_2$ were purchased from Sigma-Aldrich. All the Cyclic Voltammogram (CV) experiment were carried out inside an Mbraun glove box (O_2 < 0.1 ppm, H_2O = 0.3 ppm) using anhydrous inhibitor-free THF containing 0.1 M nBu_4NPF_6 as solvent using a IJ-Cambria CHI-660 potentiostat. Glassy carbon disks (3 mm diameter) were used as working electrode, Pt wire as counter electrode and an Ag wire as a quasireference electrode. The CVs were run at 100 mVs^{-1} scan rate and the potentials were referred to ferrocene, added at the end of each experiment and subsequently converted to NHE.

Formatted: Highlight

Reaction of Ni(6-Mes)(PPh_3)Br with O_2. A THF (15 mL) solution of Ni(6-Mes)(PPh_3)Br (140 mg, 0.194 mmol) in an ampule fitted with a J. Youngs resalable PTFE valve was freeze-pump-thaw degassed three times and the yellow solution exposed to 1 atm of O_2, leading to the instantaneous formation of a purple colored solution. After

stirring for 5 min, the solvent was removed under vacuum, the residue washed with hexane (10 mL) and then dissolved in C_6H_5F (10 mL). Hexane (20 mL) was added with vigorous stirring to yield a purple microcrystalline solid. Combined yield of **3** and **5**: 47.5 mg. Crystals of **3** appropriate for both X-ray and elemental analysis were grown from THF/hexane. Anal. Calcd. (found) for **3**, $C_{44}H_{56}N_4O_2Br_2Ni_2$ (%): C 55.62 (55.39), H 5.94 (5.94), N 5.90 (5.85).

Reaction of Ni(7-Mes)(PPh_3)Br with O_2. As above, but with Ni(7-Mes)(PPh_3)Br (162 mg, 0.220 mmol). Combined yield of **4** and **6**: 56.5 mg. X-ray quality crystals of **4** (which were also used for microanalysis) were grown from CH_2Cl_2/hexane. Anal. Calcd. (found) for **4**, $C_{46}H_{60}N_4O_2Br_2\ Ni_2$ (%): C 55.62 (56.29), H 5.94 (5.97), N 5.90 (5.87).

Ni(6-MesDAC)(PPh_3)Br (7). A THF (20 mL) solution of free 6-MesDAC (386 mg, 1.02 mmol) was added to a mixture of $Ni(cod)_2$ (139 mg, 0.50 mmol) and $Ni(PPh_3)_2Br_2$ (381 mg, 0.51 mmol). The mixture was stirred at room temperature for 2.5 h to afford a dark orange solution. After filtration, the filtrate was concentrated and hexane (20 mL) added to precipitate a dark purple solid, which was filtered, washed with hexane (10 mL) and dried in vacuo. Yield: 490 mg (62 %). Analytically pure **7** was obtained by recrystallization from C_6H_6/hexane. Anal. Calcd. (found) for $C_{42}H_{43}N_2O_2PBrNi$ (%): C 64.89 (64.61), H 5.58 (5.39), N 3.60 (3.41).

Reactivity of 7 with O_2. A THF (10 mL) solution of Ni(6-MesDAC)(PPh_3)Br (79 mg, 0.10 mmol) was free-pump-thaw degassed (3 cycles) and the solution opened to 1 atm O_2. A color change from dark orange-red to nearly colorless ensued in < 1 min. After stirring for 5 min, the solution was reduced to dryness, and the residue washed with hexane (10 mL) to afford a dark yellow material. Recrystallization from CH_2Cl_2/hexane

generated 22 mg of a mixture of $Ni(O=PPh_3)_2Br_2$ (green crystals) and (6-MesDAC)=O (colorless crystals). ^1H NMR (400 MHz, CD_2Cl_2, 25°C): δ 7.82 (br s), 7.03 (br s), 6.72* (s, 4H), 2.07* (s, 12H), 2.05* (s, 6H), 1.61* (s, 6H). The resonances marked * match with those reported for (6-MesDAC)=O.[19]

Ni(6-*o*-Tol)(PPh$_3$)Br (8). [6-*o*-Tol]BF_4 (153 mg, 0.58 mmol) and K[$N(SiMe_3)_2$] (116 mg, 0.58 mmol) were dissolved in THF (15 mL) and left stirring for 30 min. After cannula transfer to a mixture of $Ni(cod)_2$ (80 mg, 0.29 mmol) and $Ni(PPh_3)_2Br_2$ (215mg, 0.29 mmol), the solution was left stirring at room temperature for 2 h to afford a dark yellow solution. Cannula filtration and addition of hexane (20 mL) gave a yellow precipitate, which was filtered, washed with hexane (10 mL) and dried under vacuum. Analytically pure product was achieved upon recrystallization from C_6H_6/hexane. Yield: 220 mg (57 %). Anal. Calcd. (found) for $C_{36}H_{35}BrN_2NiP$ (%): C 65.00 (64.81), H 5.30 (5.21), N 4.21 (4.35).

Ni(6-*o*-Tol)(PPh$_3$)Br$_2$ (10). Exposure of a freeze-pump-thaw degassed (three cycles) THF solution (10 mL) of Ni(6-*o*-Tol)(PPh_3)Br (41 mg, 0.062 mmol) to 1 atm of O_2 led to an instantaneous color change from yellow to purple/red. Removal of the solvent in vacuo gave a purple/red residue, which was washed with hexane (10 mL), dissolved in C_6H_5F (10 mL) and layered with hexane (20 mL) to give **10** as a purple microcrystalline solid. Yield: 9 mg (20 %). Alternatively, a toluene solution (20 mL) of 6-*o*-Tol (prepared in-situ by reaction of the pyrimidinium salt [6-*o*-TolH]BF_4 (345 mg, 1.30 mmol) and $KN(SiMe_3)_2$ (257 mg, 1.29 mmol)) was added to a toluene solution (10 mL) of $Ni(PPh_3)_2Br_2$ (959 mg, 1.29 mmol). The mixture was stirred at room temperature for 1 h to give a dark purple solution. After cannula filtration, the volatiles were removed

under vacuum and the residue washed with hexane (15 mL). The resulting purple-green residue was recrystallized repeatedly from toluene/hexane to remove all traces of [6-*o*-TolH][Ni(PPh_3)Br_3] (see ESI) and leave just **10**. Yield 141 mg (15%). $^{31}P\{^1H\}$NMR (162 MHz, CD_2Cl_2, 25°C): δ 17.3 (s), 16.6 (s). $^{13}C\{^1H\}$ NMR (126 MHz, CD_2Cl_2, 25°C): δ 194.1 (d, $^2J_{CP}$ = 122 Hz, N*C*N), 193.7 (d, $^2J_{CP}$ = 123 Hz, N*C*N), 146.3 (s, N-*C*), 145.9 (s, N-*C*), 137.7 (s), 136.9 (s), 135.2 (br m), 132.9 (s), 132.6 (s), 131.9 (s), 131.7 (s) 129.7 (s), 128.6 (s), 128.4 (s), 127.8 (s), 127.7 (s), 127.0 (s), 126.7 (s,), 49.4 (s, N*C*H_2), 49.0 (s, N*C*H_2), 21.3 (s, NCH$_2$*C*H_2), 20.2 (s, *o*-*C*H_3), 19.8 (s, *o*-*C*H_3). Anal. Calcd. (found) for $C_{36}H_{35}N_2PBr_2Ni$ (%): C, 58.03 (57.85), H 4.73 (4.83), N 3.76 (3.69).

Ni(7-*o*-Tol)(PPh_3)Br_2 (11). As for **10**, by reaction of Ni(7-*o*-Tol)(PPh_3)Br (47 mg, 0.069 mmol) with O_2 to give 10 mg (38 %) of **11**. The alternative route to **10** could also be applied to **11** starting with Ni(PPh_3)$_2Br_2$ and addition of a toluene solution (20 mL) of 7-*o*-Tol (prepared in-situ by reaction of [7-*o*-TolH]BF_4 (200 mg, 0.55 mmol) with KN($SiMe_3$)$_2$ (110 mg, 0.55 mmol)) to a toluene solution (5 mL) of Ni(PPh_3)$_2Br_2$ (406 mg, 0.55 mmol). Yield: 47 mg (12 %). $^{31}P\{^1H\}$NMR (162 MHz, $CDCl_3$, 25°C): δ 21.4 (s), 21.3 (s), 20.3 (s), 17.5 (s), 16.7 (s). $^{13}C\{^1H\}$ NMR (100 MHz, C_6D_6, 25°C): δ 206.7 (d, $^2J_{CP}$ = 123 Hz, N*C*N), 148.7 (s), 147.4 (s), 147.1 (s), 137.4 (s), 137.2 (s), 135.6 (s), 135.5 (s), 133.0 (s), 131.6 (s), 129.2 (s) 127.6 (d, J_{CP} = 9 Hz), 126.7 (s), 56.0 (s, N*C*H_2), 55.9 (s, N*C*H_2), 55.7 (s, N*C*H_2), 55.6 (s, N*C*H_2), 25.5 (s, NCH$_2$*C*H_2), 23.7 (s, NCH$_2$*C*H_2), 21.4 (s, *o*-*C*H_3), 20.8 (s, *o*-*C*H_3), 20.6 (s, *o*-*C*H_3), 20.1 (s, *o*-*C*H_3). Yield 48 mg (12%). Anal. Calcd (found) for $C_{37}H_{37}N_2PBr_2Ni$ (%): C, 58.69 (58.54), H 4.93 (5.05), N 3.69 (3.60).

X-ray Crystallography. Single crystals of compounds for **3**-**5**, **7**, **10** and **11** were analysed using a Nonius Kappa CCD diffractometer. Data were collected at -123°C

using Mo($K\alpha$) radiation throughout. Details of the data collections, solutions and refinements are given in Table 1. The structures were solved using SHELXS-97[20] and refined using full-matrix least squares in SHELXL-97.[20] Refinements were generally straightforward and notable points follow.

The hydrogen atoms on the hydroxyl groups in **3** and **4** were readily located and refined at distances of 0.9 and 0.98 Å from the relevant parent oxygen atoms, respectively, in these structures. Halide disorder (80:20 ratio) of chloride versus bromide was accommodated in the model for **5**. The ADPs for the associated pairs of fractional-occupancy atoms, at each ligand site, were refined subject to being similar. In **10**, the tolyl ring based on C(12) exhibited disorder in a 75:25 ratio. To assist convergence in the latter structure, the arising fractional occupancy rings were refined as rigid hexagons and ADP restraints were also applied. It is likely that there is also some similar disorder associated with the tolyl ring based on C(5) in this structure but, despite copius efforts, a model to further resolve this region of the electron density map could not be attained.

Crystallographic data for compounds **3**-**5**, **7**, **10**, **11** and $Ni(O{=}PPh_3)_2Br_2$ (ESI only) have been deposited with the Cambridge Crystallographic Data Centre as supplementary publications CCDC 972766 (**3**), 972767 (**4**), 972768 (**5**), 972769 (**7**), 905841 (**10**), 905840 (**11**) and 974548 ($Ni(O{=}PPh_3)_2Br_2$). Copies of the data can be obtained free of charge on application to CCDC, 12 Union Road, Cambridge CB2 1EZ, UK [fax(+44) 1223 336033, e-mail: deposit@ccdc.cam.ac.uk].

Results and Discussion

Conversion of Ni(6-/7-Mes)(PPh_3)Br to Ni(II) Dimers With Oxidized N-Mes Ligands. Addition of 1 atm O_2 to yellow THF solutions of either Ni(6-Mes)(PPh_3)Br (**1**) or Ni(7-Mes)(PPh_3)Br (**2**) led to instantaneous color changes to purple. Upon removal of the solvent and recrystallization of the resulting residues from fluorobenzene/hexane, purple crystals of Ni(6-Mes)(Br)(μ-OH)(μ-O-6-Mes′)NiBr (**3**) and Ni(7-Mes)(Br)(μ-OH)(μ-O-7-Mes′)NiBr (**4**) were isolated (Scheme 1). Both products result from the oxidation of a C-H bond of one of the *ortho*-methyl groups on the NHCs and comprize of Ni(II) dimers with bridging aryloxy and hydroxy ligands. The most likely source of hydrogen in the latter is the oxidized methyl arm of the carbene.[8]

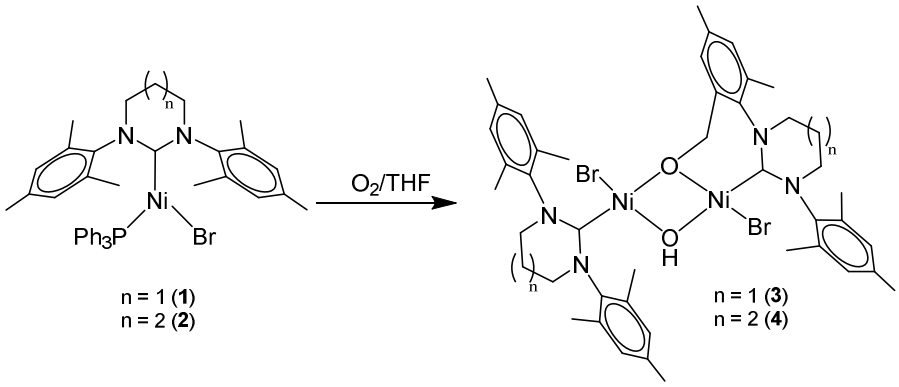

Scheme 1

The X-ray crystal structures of **3** and **4** are shown in Figure 1. In both cases, the four-coordinate Ni centers display distorted square planar geometries. This may reflect the strain imposed by the bridging OCH_2-aryl group, which contributes to some acute O-Ni-O bond angles (**3**: 80.18(10), 80.55(10)°; **4**: 80.13(13), 79.40(13)°). The Ni-O distances in the central Ni_2(μ-OR)(μ-OH) units are also asymmetric; the longest distances are found between the non-oxidized NHC bound Ni and μ-OCH_2-aryl (**3**:

Ni(1)-O(1) 1.926(2) Å; **4**: Ni(2)-O(1) 1.936(3) Å), the shortest Ni-O bond lengths being from the same Ni centers to the μ-OH groups (**3**: Ni(1)-O(2) 1.869(3) Å; **4**: Ni(2)-O(2) 1.878(4) Å). It is notable that, in **3**, deviation of the carbene nitrogen atoms from the mean plane of the surrounding bonded carbon atoms is maximized in the case of that bonded to the hydroxylated mesityl ring (0.11 Å for N(3) relative to an average of 0.02 Å for N(4), N(5) and N(6). These data reflect a distortion from idealized sp^2 geometry at N(3), about which, strain is optimal. A comparative observation is evident in **4** where the distance of N(2) from the mean plane of the surrounding bonded carbon atoms is 0.16 Å.

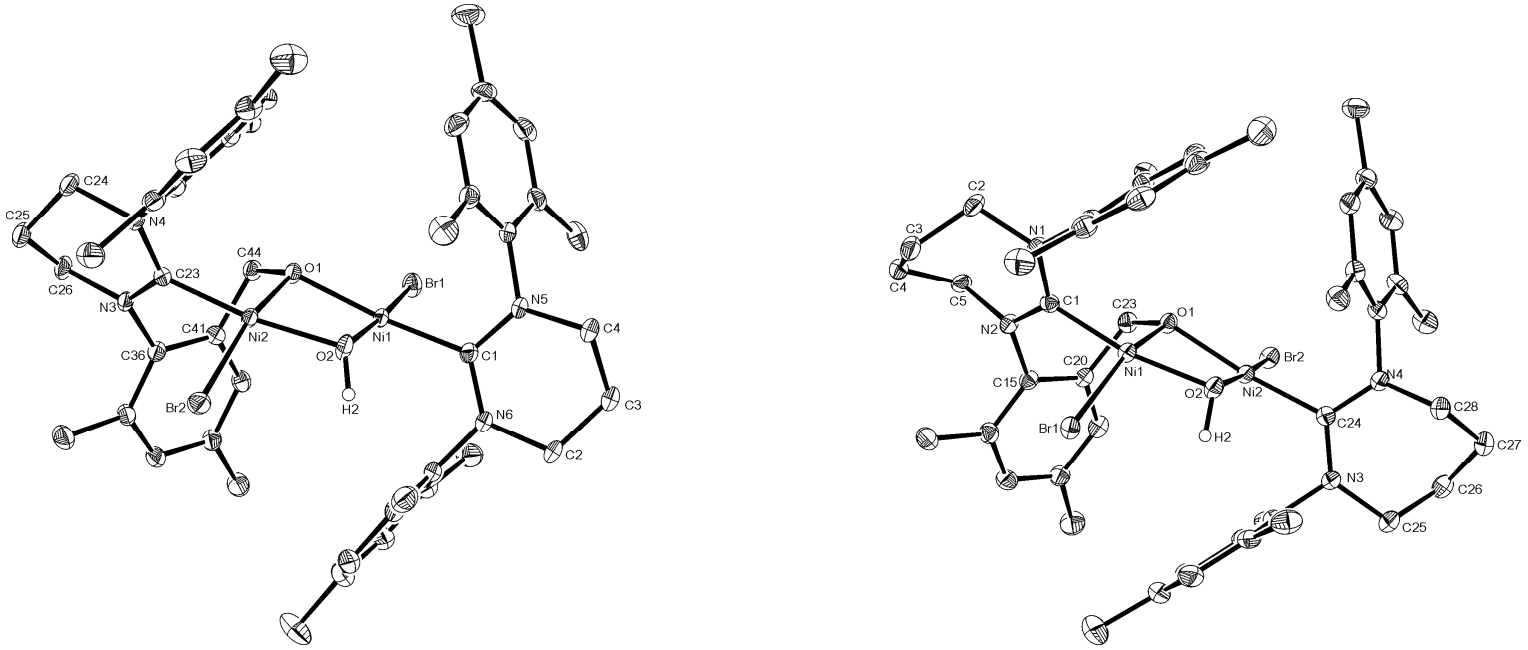

Figure 1. Molecular structures of **3** (left) and **4** (right). Ellipsoids are shown at the 30% level. Hydrogen atoms except for μ-OH are removed for clarity. Selected bond lengths (Å) and angles (°) in **3**: Ni(1)-C(1) 1.883(4), Ni(2)-C(23) 1.856(3), Ni(1)-O(1) 1.926(2), Ni(1)-O(2) 1.869(3), Ni(2)-O(1) 1.892(2), Ni(2)-O(2) 1.890(2), O(1)-C(44) 1.443(4), Ni(1)-O(1)-Ni(2) 97.53(11), O(1)-C(44)-C(41) 111.4(3). Selected bond lengths (Å) and angles (°) in **4**: Ni(1)-C(1) 1.878(4), Ni(2)-C(24) 1.896(4), Ni(1)-O(1) 1.889(3), Ni(1)-O(2) 1.896(3), Ni(2)-O(1) 1.936(3), Ni(2)-O(2) 1.878(3), O(1)-C(23) 1.437(5), Ni(1)-O(1)-Ni(2) 98.00(13), O(1)-C(23)-C(20) 112.6(4).

Additional characterization of **3** and **4** was provided by NMR and IR spectroscopy. Although the carbene region of the ^{1}H NMR spectrum of **3** was largely uninformative due to the presence of quite broad, overlapping resonances (see ESI), the hydroxyl group was apparent as a singlet at δ -8.21 (THF-d_8).[21] By IR spectroscopy, a μ-OH stretch appeared at 3412 cm^{-1}. Both NMR and IR signals disappeared upon addition of D_2O. The ^{1}H NMR spectrum of **4** in C_6D_6 showed two Ni-OH resonances at δ -8.37 and -9.02, which we believe arise from different conformers of the product (c.f. **10** below). Shaking with D_2O removed both OH resonances, along with a μ-OH IR absorption band at 3437 cm^{-1}. Neither **3** nor **4** were soluble enough in a range of solvents (acetone, acetonitrile, benzene, toluene, dichloromethane, C_6H_5F) to allow observation of the Ni-C_{NHC} resonances by $^{13}C\{^{1}H\}$ NMR. Complex **3** proved to be soluble in neat pyridine or in pyridine doped CH_2Cl_2 (5 equiv C_5H_5N) with the formation of orange solutions; layering a sample in CH_2Cl_2/C_5H_5N with hexane afforded a small number of purple crystals, which upon analysis by X-ray crystallography (Figure 2), were found to be the doubly oxidized Ni(II) product Ni(Br)(μ-O-6-Mes′)$_2$NiBr (**5**). The coordination spheres of the two identical square planar Ni centers consisted of an oxidized 6-Mes ligand, two μ-OR linkages and 80:20 mixture of disordered Br and Cl ligands, the latter presumably arising from the CH_2Cl_2 solvent. The oxidized arms of the 6-Mes ligands were in a *syn* arrangement about the planar $Ni_2(\mu\text{-OR})_2$ core with Ni-O distances comparable to those in **3**. In contrast to **3** and **4**, structural distortions of the nitrogen atoms attached to the oxidized mesityl group were marginal.

During (unsuccessful) attempts to generate **5** in higher yield for more complete characterization, we showed that ESI-QTOF mass spectrometry of MeCN solutions of

microcrystalline material precipitated from the reaction of **1** with O_2 gave an isotope pattern consistent with the formation of both **3** and **5** in the initial O_2 activation reaction (this was also the case for **4** and the doubly oxidized analogue **6**: see ESI for mass spectra).[22] Indeed, integration of the ^{1}H NMR spectrum relative to the Ni-OH resonance at δ -8.21 showed clearly that there were too many protons than could be accounted for by the presence of just **3** alone.

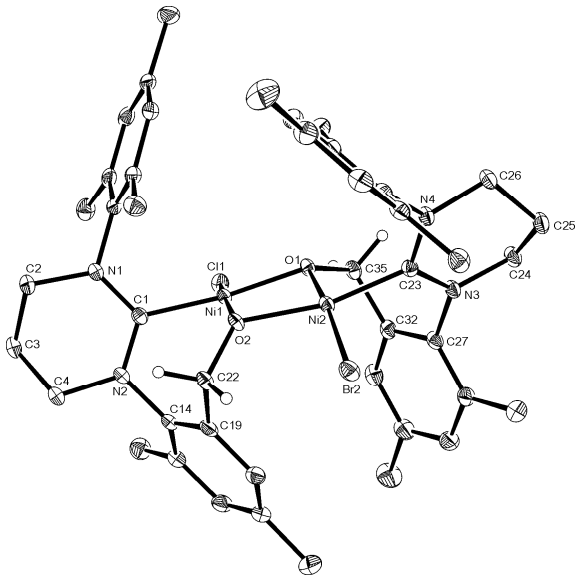

Figure 2. Molecular structure of **5**. Ellipsoids are shown at the 30% level. Hydrogen atoms (except for those on the oxidized methyl arms) are removed for clarity. Selected bond lengths (Å) and angles (°): Ni(1)-C(1) 1.868(2), Ni(2)-C(23) 1.872(2), Ni(1)-O(1) 1.9204(14), Ni(1)-O(2) 1.8806(15), Ni(2)-O(1) 1.8873(14), Ni(2)-O(2) 1.9166(14), Ni(1)-O(1)-Ni(2) 99.48(6), Ni(1)-O(2)-Ni(2) 99.86(7).

UV-Visible Spectroscopic Studies on the Reaction of 1 with O_2. The room temperature electronic absorption spectrum of **3** in THF solution contained a single absorption band at λ_{max} = 362 nm with ε = 474 M cm^{-1}. In an effort to probe the mechanism of formation of **3** in more detail, complex **1** was dissolved in THF at -83 ^{o}C and 1 mL of air was added at this temperature. The color of the solution changed from light orange to purple and the reaction was monitored by UV-vis spectroscopy as displayed in Figure 3. After 6 min reaction time, no further change was observed in the UV-vis revealing that the reaction was complete. The final spectrum obtained is very similar to that of μ-alkoxy/μ-hydroxy complex **3** suggesting that this is the major species of the reaction of (**1** + O_2). However, it is likely that the bis-μ-alkoxy complex **5** would have a very similar UV-vis spectrum due to the very similar chromophores. Indeed, evidence for the formation of multiple species was suggested by the kinetic analysis where the singular value decomposition (SVD) analysis shows the presence of at least three eigenvectors. It is therefore not possible to develop a simple kinetic model even if at first sight nice isosbestic points are observed at 290 and 420 nm.

The formation of **3** from **1** and oxygen suggest the formation of highly reactive high oxidation state Ni bis-oxo or peroxo species that further evolve towards the formation of **3** and **5**.[23] Attempts to detect such intermediates by carrying out the reaction at different temperatures were unsuccessful.

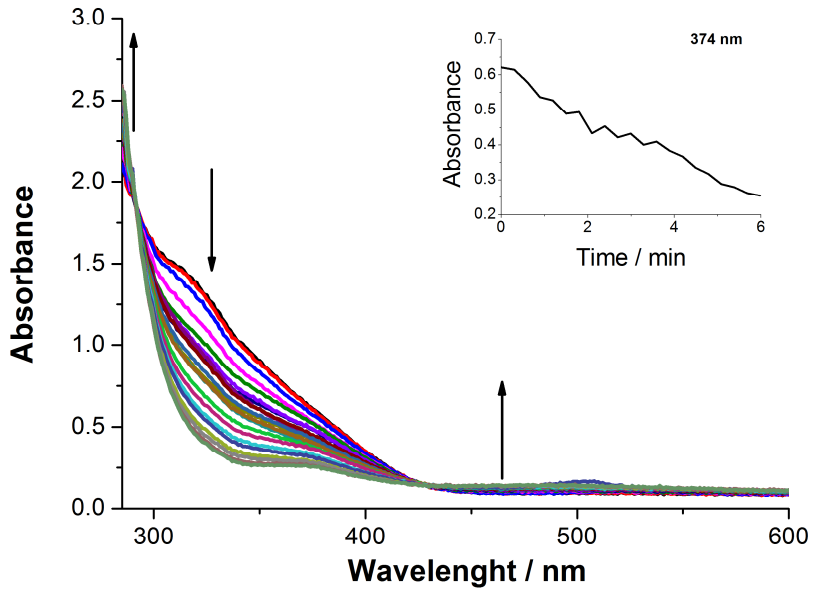

Figure 3. UV-vis monitoring of the reaction of 1 mL of air with 0.5 mM **1** at -83 ^{o}C in THF over a period of 6 min. Measurements were taken every 18 s. The inset shows the abs vs time plot at 374 nm.

Synthesis and Reactivity Towards O_2 of Ni(6-MesDAC)(PPh_3)Br (7). In an attempt to retard the rate of mesityl group oxidation, the reactivity of the less electron-rich diamidocarbene[24] complex Ni(6-MesDAC)(PPh_3)Br (**7**) was probed. Employing the same approach used for the synthesis of **1** and **2**, a comproportionation reaction of $Ni(cod)_2$ and $Ni(PPh_3)_2Br_2$ in the presence of free 6-MesDAC gave the purple Ni(I) product **7**, which was isolated in 60% yield (Scheme 2).

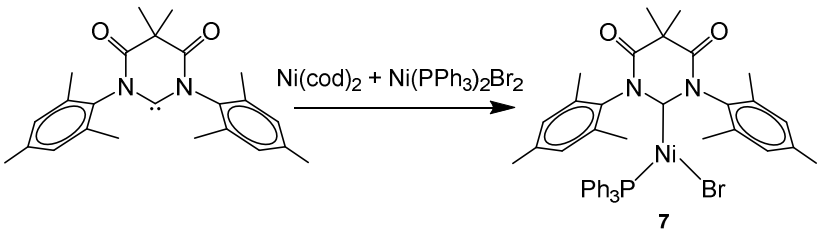

Scheme 2

The spectroscopic properties of **7** were in agreement with those found for **1** and **2**, namely a series of broad resonances between δ 11 and -1 in the proton NMR spectrum, and no sign of any signal in the $^{31}P\{^{1}H\}$ spectrum. Likewise, the X-ray structure of **7** (Figure 4) was isostructural with that of **1**. There was a significant shortening of the Ni-C bond length relative to that in **1** (1.8702(18) Å c.f. 1.942(2) Å), presumably resulting from the enhanced π-acceptor character of the amidocarbene.[23]

An immediate but quite different color change took place upon addition of O_2 to a THF solution of **7** (purple crystals of **7** dissolved to give dark orange-yellow solutions, which became virtually colorless upon addition of O_2), suggestive of the formation of quite different products to **3** and **4**. Indeed, crystallization from either CH_2Cl_2/hexane or THF/hexane afforded a mixture of green and colorless crystals, which upon manual separation and analysis by a combination of X-ray crystallography and NMR spectroscopy were shown to be the Ni(II) phosphine oxide complex $Ni(O{=}PPh_3)_2Br_2$ (see ESI for structure)[25] and urea (6-MesDAC)=O respectively.[19]

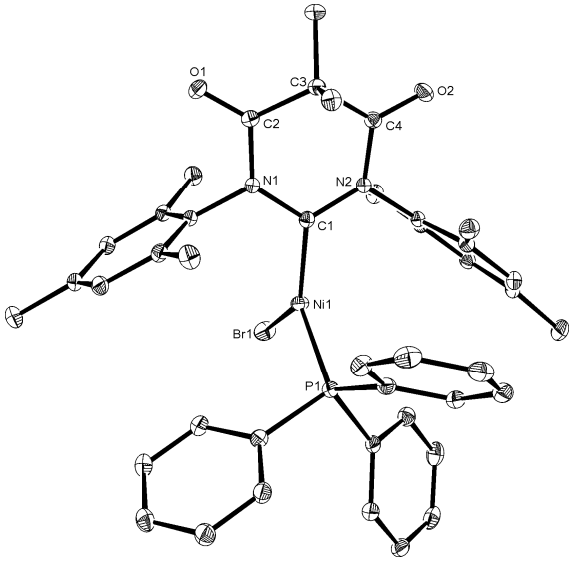

Figure 4. Molecular structure of **7**. Ellipsoids are shown at the 30% level. All hydrogen atoms are removed for clarity. Selected bond lengths (Å) and angles (°): Ni(1)-C(1) 1.8702(18), Ni(1)-P(1) 2.2614(5), Ni(1)-Br(1) 2.3029(3), C(1)-Ni(1)-P(1) 118.99(5), C(1)-Ni(1)-Br(1) 127.66(5), P(1)-Ni(1)-Br(1) 113.352(16).

Reactivity of Ni(6-/7-*o*-Tol)(PPh_3)Br_2 with O_2. Sparging THF solutions of the less bulky N-*ortho*-tolyl substituted carbene containing complexes Ni(6-*o*-Tol)(PPh_3)Br (**8**) and Ni(7-*o*-Tol)(PPh_3)Br (**9**) with O_2 failed to bring about oxidation of the NHC ligands. Instead, metal oxidation along with halide redistribution took place to afford the mixed NHC-phosphine Ni(II) complexes Ni(6-/7-*o*-Tol)(PPh_3)Br_2 (**10**, **11**) (Scheme 3). The products could be accessed far more straightforwardly by treating $Ni(PPh_3)_2Br_2$ with 1 equiv of the corresponding *in-situ* generated NHC, although this also generated the corresponding pyrimidinium salts of $[Ni(PPh_3)Br_3]^-$ in significant amounts (see ESI for characterization).[26]

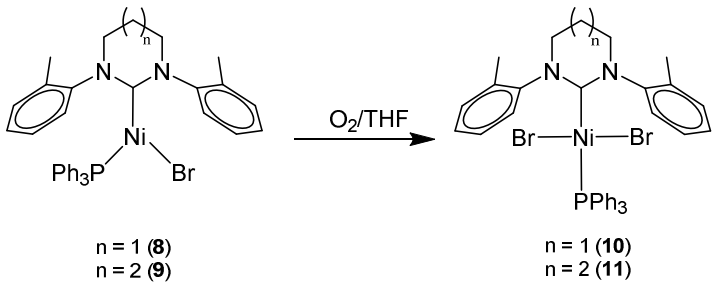

Scheme 3

The crystal structures of **10** and **11** displayed the expected square planar Ni geometries with *trans* bromide ligands (Figure 5). The Ni-C_{NHC} distances of 1.910(5) Å (**10**) and 1.905(3) Å (**11**) were comparable to the value reported in *trans*-Ni(IPr)(PPh_3)Cl_2 (IPr = 1,3-bis(2,6-diisopropylphenyl)imidazol-2-ylidene),[27] which is one of the few other reported Ni(NHC)(PR_3)(halide)$_2$ complexes. Neither **10** nor **11** showed the expected single $^{31}P\{^1H\}$ NMR resonances; two resonances (ratio ca. 1:1.5) were observed for **10** (CD_2Cl_2: δ 17.3 and 16.6) and five resonances for **11**, although two signals predominated (C_6D_6: δ 21.4, 21.3, 20.3, 17.5, 16.7 in approximate ratio of 1:2:1:38:13). An explanation based on the presence of *cis*-/*trans*-isomers was ruled out for **10** by the presence of large (122 Hz) *trans*-$^{13}C/^{31}P$ couplings on both of the carbene resonances observed in the $^{13}C\{^1H\}$ NMR spectrum. Whereas the $^{31}P\{^1H\}$ spectrum of **10** was unchanged between 272-332 K, that of **11** showed four much broader peaks at 332 K, but five signals upon cooling back to ambient temperature. A ^{31}P-^{31}P EXSY experiment on **11** revealed room temperature exchange between the resonances at δ 17.5

and 16.7, and a separate exchange process involving the three signals at δ 21.4, 21.3 and 20.3 (see ESI).

The existence of rotamers affords the most likely explanation for the multiple phosphorus signals. Cavell's group have proposed rotamers (differing in *syn*- versus *anti*-arrangements of the *o*-Me groups of an NHC) to account for the appearance of the NMR spectra of the isoelectronic Rh(7-*o*-Tol)(cod)Cl.[28]

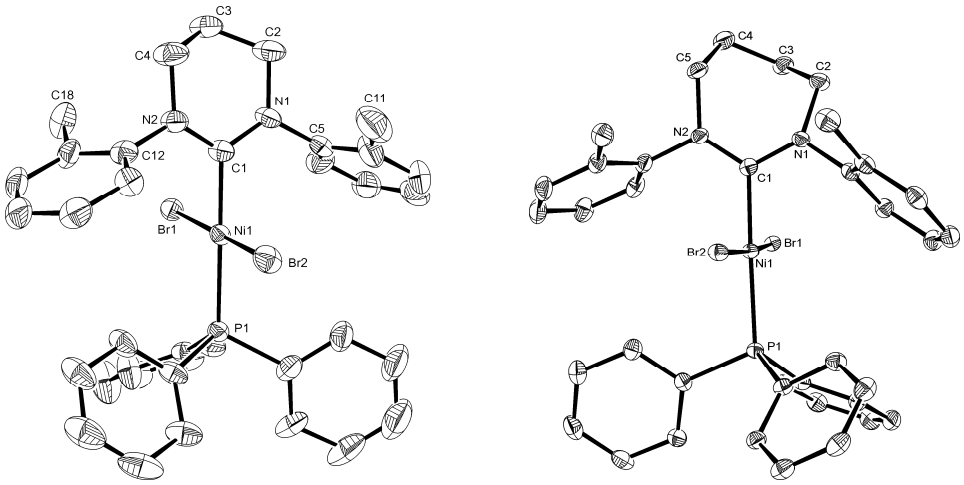

Figure 5. Molecular structures of **10** (left) and **11** (right). Ellipsoids are shown at the 30% level. Hydrogen atoms are removed for clarity. Selected bond lengths (Å) and angles (°) in **10**: Ni(1)-C(1) 1.910(5), Ni(1)-P(1) 2.2505(15), Ni(1)-Br(1) 2.3026(8), Ni(1)-Br(2) 2.3122(9), C(1)-Ni(1)-P(1) 179.26(18), Br(1)-Ni(1)-Br(2) 175.82(4). Selected bond lengths (Å) and angles (°) in **11**: Ni(1)-C(1) 1.905(3), Ni(1)-P(1) 2.2615(8), Ni(1)-Br(1) 2.4013(4), Ni(1)-Br(2) 2.3511(4), C(1)-Ni(1)-P(1) 177.44(9), Br(1)-Ni(1)-Br(2) 174.192(19).

Redox Properties of Mononuclear Complexes. The redox properties of Ni(I) mononuclear complexes **1-2** and **7-9**, were investigated by means of cyclic voltammetry and the results obtained are reported in Figure 6 and the supporting information section.

Figure 6 shows the CV of complexes **1** and **9** where a chemically irreversible oxidation can be observed in the anodic region and a chemically irreversible one can be found in the cathodic region.

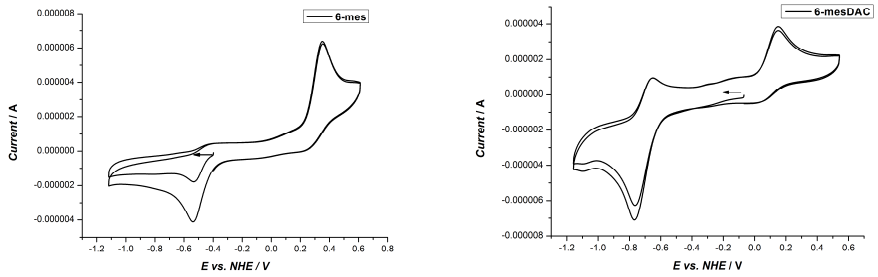

Figure 6. Cyclic voltammograns for complexes **1** (solid line) and **9** (dashed line) at 100 mV/s scan rate *vs.* NHE. The arrow indicates the initial scanning potential and the scan direction.

A similar behavior is observed for the other complexes studied except for **7** and **8** that show two irreversible reductions. All the $E_{p,a}$ and $E_{p,c}$ found for these complexes are reported in Table 2. As already mentioned, in all cases the processes are chemically irreversible and this precludes the extraction of accurate thermodynamic potentials. However since all the mononuclear complexes studied here have a very similar molecular structure, especially around the Ni metal center, an indicative trend can be deduced.

Formatted: Highlight
Formatted: Left, Indent: First line: 1,27 cm
Formatted: Font: Not Bold
Formatted: Font: Not Bold
Formatted: Font: Bold
Formatted: Font: Bold
Formatted: Font: Bold
Formatted: Left
Formatted: Pattern: Clear (White)
Formatted: Pattern: Clear (White), Not Highlight
Formatted: Font: Bold, Pattern: Clear (White), Not Highlight
Formatted: Font: Bold
Formatted: Font: Italic, Pattern: Clear (White), Not Highlight
Formatted: Pattern: Clear (White), Not Highlight
Formatted: Left, Indent: First line: 1,27 cm
Formatted: Indent: First line: 1,27 cm
Formatted: Font: Bold
Formatted: Font: Bold
Formatted: Font: Italic
Formatted: Font: Italic, Subscript
Formatted: Font: Italic
Formatted: Font: Italic, Subscript
Formatted: Left, Indent: First line: 1,27 cm

The anodic potentials shown in Table 2, do not follow a regular trend based on the induction effects expected by increasing the number of methylene units in the carbene ligand backbone or by increasing the number of Me units in the N-substituted groups. It is also surprising that **9**, containing the amidocarbene group, displays one of the lowest $E_{p,a}$ values together with **8**. However, the most interesting feature that can be extracted from Table 2, is the fact that complexes **1** and **2** that have the highest redox potentials by far undergo oxidation involving O-atom transfer from O_2. On the other hand the rest of the complexes with much lower redox potentials undergo oxidation primarily by outer sphere electron transfer (OSET) giving basically Ni(II) complexes with no oxygen involved in the final products. This suggests that complexes that are much more difficult to oxidize by OSET (**6** and **7**) find a lower energy pathway involving O-atom transfer from O_2, hence the formation of the hydroxo-aryloxy briged Ni(II) complexes.

Formatted: Font: Not Bold
Formatted: Normal, Indent: First line: 1,27 cm, Line spacing: Double
Formatted: Font: Not Bold
Formatted: Font: Bold
Formatted: Font: Italic
Formatted: Font: Italic, Subscript
Formatted: Font: Bold
Formatted: Font: Bold
Formatted: Font: Bold
Formatted: Subscript
Formatted: Font: Bold
Formatted: Font: Bold
Formatted: Subscript
Formatted: Left
Formatted: Left, Indent: First line: 1,27 cm

Summary and Conclusions

A series of three-coordinate Ni(NHC)(PPh_3)Br complexes have been shown to react very readily with O_2 to afford products that are dependent upon the nature of the carbene. Bulky, 6- or 7-membered ring N-mesityl substituted NHCs lead to oxidation of the carbene and formation of dimeric Ni(II) products with μ-alkoxy ligands, whereas less bulky N-*o*-Tol derived analogues react to give the simple Ni(II) dibromido complexes Ni(NHC)(PPh_3)Br_2. Changing from a diamino to a diamidocarbene afforded isolable products that result from Ni-carbene cleavage and NHC/phosphine oxidation.

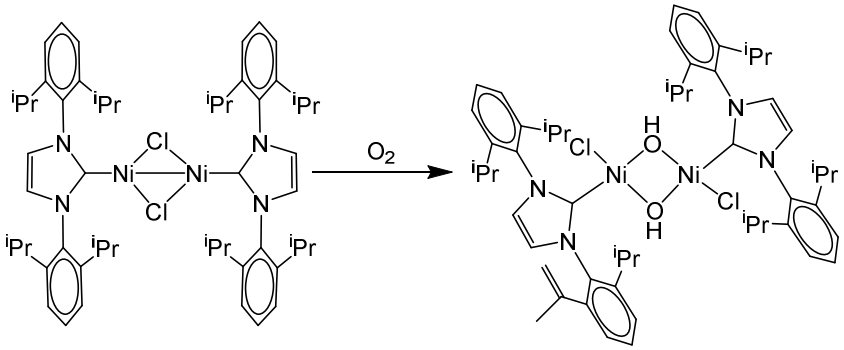

Scheme 4

Our results show some parallels to previous studies from Sigman's group,[13a,21c,29] who reported that addition of O_2 to a Ni(I) dimer with large IPr ligands (Scheme 4) resulted in oxidation of an N-dipp group, albeit through dehydrogenation rather than hydroxylation of an ^{i}Pr substituent. Addition of O_2 to the Ni(II) allyl complexes Ni(NHC)(η^3-C_3H_5)Cl containing bulky IPr, SIPr or IMes groups[30] produced the parent, non-dehydrogenated bis-μ-OH dimers [Ni(NHC)Cl]$_2$(μ-OH)$_2$, whereas the

use of less congested NHCs resulted in similar ligand rearrangement reactions to those observed by us; for example, Ni(I-*p*-Tol)(η^3-C_3H_5)Cl was converted to Ni(I-*p*-Tol)$_2$Cl$_2$.[29,30] Neither electronics nor sterics alone adequately explained the product distributions, but some correlation was drawn to the degree of Ni-NHC bond rotation, which impacted upon the ability of O_2 to approach and coordinate to Ni(NHC)(η^3-C_3H_5)Cl in the first instance. The range of products that we observe upon changing N-Mes to N-*o*-Tol substituents and diamino to diamido carbenes similarly points to a role for both sterics and electronics. However, until we can find a method to slow down the rates of reaction with O_2 and/or generate only single products, it is unlikely that we will be able to extract any mechanistic details that will prove to be that informative.

Acknowledgement. We acknowledge the University of Bath (Excellent Studentship Award) and MINECO (CTQ2010-21497) for financial support. Dr Anneke Lubben and Dr John Lowe are thanked for help with mass spectrometry and NMR respectively, while Mr Lee Collins is thanked for samples of 6-MesDAC.

Supporting Information Available: NMR mass spectrometry data for **3-6**, X-ray structure of Ni(O=PPh$_3$)$_2$Br$_2$**,** characterization of [6-*o*-TolH][Ni(PPh$_3$)Br$_3$] and EXSY data for **11**. This material is available free of charge via the Internet at http://pubs.acs.org.

.

References

1. (a) Ito, M.; Kotera, M.; Matsumoto, T.; Tatsumi, K. *Proc. Natl. Acad. Sci. USA* **2009**, *106*, 11862. (b) Horn, B.; Limberg, C.; Herwig, C.; Mebs, S. *Angew. Chem. Int. Ed.* **2011**, *50*, 12621.

2. (a) Dobbek, H.; Svetlitchnyi, V.; Gremer, L.; Huber, R.; Meyer, O. *Science* **2001**, *293*, 1281. (b) Doukov, T. I.; Iverson, T. M.; Seravalli, J.; Ragsdale, S. W.; Drennan, C. L. *Science* **2002**, *298*, 567.

3. (a) Fontecilla-Camps, J. C.; Volbeda, A.; Cavazza, C.; Nicolet, Y. *Chem. Rev.* **2007**, *107*, 4273. (b) Ogata, H.; Lubitz, W.; Higuchi, Y. *Dalton Trans.* **2009**, 7577.

4. (a) Youn, H. D.; Kim, E. J.; Roe, J. H.; Hah, Y. C.; Kang, S. O. *Biochem. J.* **1996**, *318*, 889. (b) Broering, E. P.; Truong, P. T.; Gale, E. M.; Harrop, T. C. *Biochemistry* **2013**, *52*, 4.

5. (a) Pochapsky, T. C.; Pochapsky, S. S.; Ju, T.; Mo, H.; Al-Mjeni, F.; Maroney, M. J. *Nature Struct. Bio.* **2002**, *9*, 966. (b) Ju, T.; Goldsmith, R. B.; Chai, S. C.; Maroney, M. J.; Pochapsky, S. S.; Pochapsky, T. C. *J. Mol. Biol.* **2006**, *393*, 823.

6. (a) Hikichi, S.; Yoshizawa, M.; Sasakura, Y.; Akita, M.; Moro-Oka, Y. *J. Am. Chem. Soc.* **1998**, *120*, 10567. (b) Hikichi, S.; Yoshizawa, M.; Sasakura, Y.; Komatsuzaki, H.; Akita, M.; Moro-oka, Y. *Chem. Lett.* **1999**, 979. (c) Hikichi, S.; Yoshizawa, M.; Sasakura, Y.; Komatsuzaki, H.; Moro-oka, Y.; Akita, M. *Chem. Eur. J.* **2001**, *7*, 5011. (d) Cho, J.; Furutachi, H.; Fujinami, S.; Tosha, T.; Ohtsu, H.; Ikeda, O.; Suzuki, A.; Nomura, A.; Uruga, T.; Tanida, H.; Kawai, T.; Tanaka, K.; Kitagawa, T.; Suzuki, M. *Inorg. Chem.* **2006**, *45*, 2873. (e) Cho, J.; Kang, H. Y.; Liu, L. V.; Sarangi, R.; Solomon, E. I.; Nam, W. *Chem. Sci.* **2013**, *4*, 1502.

7. Itoh, S.; Bandoh, H.; Nakagawa, M.; Nagatomo, S.; Kitagawa, T.; Karlin, K. D.; Fukuzumi, S. *J. Am. Chem. Soc.* **2001**, *123*, 11168.

8. Kunishita, A.; Doi, Y.; Kubo, M.; Ogura, T.; Sugimoto, H.; Itoh, S. *Inorg. Chem.* **2009**, *48*, 4997.

9. For a general review on O_2 activation, see: Garcia-Bosch, I.; Ribas, X.; Costas, M. *Eur. J. Inorg. Chem.* **2012**, 179.

10. (a) Fujita, K.; Schenker, R.; Gu, W. W.; Brunold, T. C.; Cramer, S. P.; Riordan, C. G. *Inorg. Chem.* **2004**, *43*, 3324. (b) Kieber-Emmons, M. T.; Schenker, R.; Yap, G. P. A.; Brunold, T. C.; Riordan, C. G. *Angew. Chem. Int. Ed.* **2004**, *43*, 6716.

11. Yao, S.; Bill, E.; Milsmann, C.; Wieghardt, K.; Driess, M. *Angew. Chem. Int. Ed.* **2008**, *47*, 7110.

12. Riordan, C. G., In *Comprehensive Coordination Chemistry II*, McCleverty, J. A.; Meyer, T. J., Eds. Elsevier: Oxford, 2005; Vol. 8, pp 677-713.

13. (a) Dible, B. R.; Sigman, M. S.; Arif, A. M. *Inorg. Chem.* **2005**, *44*, 3774. (b) Company, A.; Yao, S. L.; Ray, K.; Driess, M. *Chem. Eur. J.* **2010**, *16*, 9669.

14. (a) Kieber-Emmons, M. T.; Riordan, C. G. *Acc. Chem. Res.* **2007**, *40*, 618. (b) Yao, S. L.; Driess, M. *Acc. Chem. Res.* **2012**, *45*, 276.

15. Davies, C. J. E.; Page, M. J.; Ellul, C. E.; Mahon, M. F.; Whittlesey, M. K. *Chem. Commun.* **2010**, *46*, 5151.

16. Page, M. J.; Lu, W. Y.; Poulten, R. C.; Carter, E.; Algarra, A. G.; Kariuki, B. M.; Macgregor, S. A.; Mahon, M. F.; Cavell, K. J.; Murphy, D. M.; Whittlesey, M. K. *Chem. Eur. J.* **2013**, *19*, 2158.

17. A related oxidation of an IMes ligand brought about by N_2O has recently been reported in a dinuclear Ru-NHC complex. Tskhovrebov, A. G.; Solari, E.; Scopelliti, R.; Severin, K. *Organometallics* **2012**, *31*, 7235.

18. Hudnall, T. W.; Moerdyk, J. P.; Bielawski, C. W. *Chem. Commun.* **2010**, *46*, 4288.

19. Wiggins, K. M.; Moerdyk, J. P.; Bielawski, C. W. *Chem. Sci.* **2012**, *3*, 2986.

20. Sheldrick, G. M. *Acta. Cryst.* **1990**, *467-473*, A46. Sheldrick, G. M, SHELXL-97, a computer program for crystal structure refinement, University of Göttingen, 1997.

21. (a) Carmona, E.; Marín, J. M.; Paneque, M.; Poveda, M. L. *Organometallics* **1987**, *6*, 1757. (b) Vanderlende, D. D.; Abboud, K. A.; Boncella, J. M. *Inorg. Chem.* **1995**, *34*, 5319. (c) Dible, B. R.; Sigman, M. S. *J. Am. Chem. Soc.* **2003**, *125*, 872. (d) Cámpora, J.; Palma, P.; del Río, D.; Álvarez, E. *Organometallics* **2004**, *23*, 1652.

22. In contrast to the 6-Mes complex **4**, we were unable to find an alternative synthetic route to **6**.

23. Yao, S. L.; Herwig, C.; Xiong, Y.; Company, A.; Bill, E.; Limberg, C.; Driess, M., *Angew. Chem. Int. Ed.* **2010,** 49, 7054. For a review on the insertion of metal oxo complexes into C-H bonds, see: Gunay, A.; Theopold, K. H. *Chem. Rev.* **2010**, *110*, 1060.

24. (a) César, V.; Lugan, N.; Lavigne, G. *J. Am. Chem. Soc.* **2008**, *130*, 11286. (b) Hudnall, T. W.; Bielawski, C. W. *J. Am. Chem. Soc.* **2009**, *131*, 16039. (c) César, V.; Lugan, N.; Lavigne, G., *Eur. J. Inorg. Chem.* **2010**, 361. (d) Moerdyk, J. P.;

Bielawski, C. W. *Organometallics* **2011**, *30*, 2278. (e) Blake, G. A.; Moerdyk, J. P.; Bielawski, C. W. *Organometallics* **2012**, *31*, 3373. (f) Moerdyk, J. P.; Bielawski, C. W. *Chem. Eur. J.* **2013**, *19*, 14773.

25. (a) Cotton, F. A.; Goodgame, D. M. L. *J. Am. Chem. Soc.* **1960**, *82*, 5771. (b) (b) Daniels, W. E. *Inorg. Chem.* **1964**, *3*, 1800.

26. Xu, Y. C.; Zhang, J.; Sun, H. M.; Shen, Q.; Zhang, Y. *Dalton Trans.* **2013**, *42*, 8437.

27. Matsubara, K.; Ueno, K.; Shibata, Y. *Organometallics* **2006**, *25*, 3422.

28. Iglesias, M.; Beetstra, D. J.; Kariuki, B.; Cavell, K. J.; Dervisi, A.; Fallis, I. A. *Eur. J. Inorg. Chem.* **2009**, 1913.

29. Dible, B. R.; Sigman, M. S.; Arif, A. M. *Inorg. Chem.* **2006**, *45*, 8430.

30. SIPr = 1,3-bis-(2,6-diisopropylphenyl)imidazolin-2-ylidene; IMes = 1,3-bis (2,4,6-trimethylphenyl)imidazol-2-ylidene; I-*p*-Tol = 1,3-bis-(4-trimethylphenyl)imidazol-2-ylidene.

Table 1. Crystal data and structure refinement details for compounds **3**, **4**, **5**, **7**, **10** and **11**.

	3	**4**	**5**	**7**	**10**	**11**
Chemical formula	$C_{44}H_{56}Br_2N_4Ni_2O_2$	$C_{46}H_{60}Br_2N_4Ni_2O_2$	$C_{44}H_{54}Br_{0.40}Cl_{1.60}N_4Ni_2O_2P$	$C_{42}H_{43}BrN_2NiO_2P$	$C_{36}H_{35}Br_2N_2NiP$	$C_{37}H_{37}Br_2N_2NiP$
Formula Mass	950.17	978.22	877.02	777.37	745.16	759.19
Crystal system	Monoclinic	Triclinic	Triclinic	Monoclinic	Monoclinic	Monoclinic
Space group	$P2_1/n$	$P\bar{1}$	$P\bar{1}$	$P2_1/n$	$P2_1/n$	$P2_1/c$
a/Å	14.0430(2)	12.6730(2)	12.8530(2)	11.3530(1)	14.8730(4)	18.4030(1)
b/Å	15.6560(2)	12.8470(3)	13.4070(2)	17.9990(2)	13.5120(4)	9.3870(1)
c/Å	19.5740(3)	16.0810(3)	14.8420(3)	18.3910(2)	17.3700(5)	21.3520(2)
α/°	90.00	101.027(1)	107.486(1)	90.00	90.00	90.00
β/°	90.194(1)	110.711(1)	99.498(1)	100.635(1)	109.392(2)	115.468(1)
γ/°	90.00	104.940(1)	114.349(1)	90.00	90.00	90.00
Unit cell volume/Å^3	4303.46(11)	2247.65(8)	2095.99(6)	3693.51(7)	3292.71(16)	3330.10(5)
No. of formula units per unit cell, Z	4	2	2	4	4	4
No. of reflections measured	75160	44832	34804	72526	55969	55969
No. of independent reflections	9813	10169	9558	8447	7522	7522
R_{int}	0.0883	0.0605	0.0488	0.0516	0.0760	0.0760
Final R_1 values ($I > 2\sigma(I)$)	0.0431	0.0508	0.0370	0.0309	0.0578	0.0578
Final $wR(F^2)$ values ($I > 2\sigma(I)$)	0.0848	0.1226	0.0858	0.0771	0.1399	0.1399
Final R_1 values (all data)	0.0725	0.0809	0.0542	0.0404	0.0941	0.0941
Final $wR(F^2)$ values (all data)	0.0971	0.1369	0.0935	0.0829	0.1542	0.1542
Goodness of fit on F^2	1.100	1.070	1.035	1.047	1.178	1.016

Table 2. Anodic and Cathodic Redox Waves Observed for Selected Complexes.

Complex	***$E_{p,a}$ (V vs. NHE)***	***$E_{p,c}$ (V vs. NHE)***
2	0.48	-0.49
1	0.35	-0.54
9	0.20	-0.72, -1.08
8	0.25	-0.68, -1.19
7	0.15	-0.77

Formatted: Highlight

Formatted: Highlight

Formatted: Highlight

For Table of Contents Use Only

Stereoelectronic Effects in C-H Bond Oxidation Reactions of Ni(I) N-Heterocyclic Carbene Complexes

Rebecca C. Poulten, Isidoro López, Antoni Llobet, Mary F. Mahon and Michael K. Whittlesey

Exposure of three-coordinate Ni(I) N-heterocyclic carbene complexes to O_2 results in the rapid oxidation of an N-substituent C-H bond with N-Mes substituted ligands. With less bulky *ortho*-tolyl based ligands or less electron-rich amidocarbenes, very different mononuclear Ni(II) products are formed as a result of ligand redistribution.